Quantitative Source Apportionment of Size-segregated Particulate Matter at Urbanized Local Site in Korea

Mi-Seok Oh, Tae-Jung Lee, Dong-Sool Kim[*]

Department of Environmental Science and Engineering and Center for Environmental Studies, Kyung Hee University-Global Campus, Seocheon-dong, Giheung-gu, Yongin-si, Gyeonggi-do, Republic of Korea

Abstract

The suspended particulate matter (PM) has been collected by a cascade impactor for 2 years (September 2005–September 2007) in Kyung Hee University-Global Campus located on the border of Yongin and Suwon Cites in Korea. PM was separated into 9 fractions with following aerodynamic size ranges: ST1 (> 9 μm), ST2 (5.8–9.0 μm), ST3 (4.7–5.8 μm), ST4 (3.3–4.7 μm), ST5 (2.1–3.3 μm), ST6 (1.1–2.1 μm), ST7 (0.7–1.1 μm), ST8 (0.4–0.7 μm), ST9 (< 0.4 μm). The 20 chemical species (Al, Mn, Si, Fe, Cu, Pb, Cr, Ni, V, Cd, Ba, Zn, Na^+, NH_4^+, K^+, Mg^{2+}, Ca^{2+}, Cl^-, NO_3^-, SO_4^{2-}) were analyzed by ion coupled plasma atomic emission spectrometry and ion chromatography after proper pretreatments of each sample filter. Based on the chemical information, positive matrix factorization (PMF) was used to identify size-segregated PM sources except for ST9. A total of 11 sources were identified and their contributions were intensively estimated. Further conditional probability function (CPF) was used to examine the potential location of identified sources after PMF modeling, A result of 2-year average source contribution showed that aged sea salt, road dust, long-range transport, and soil sources were most dominant in ST1 (PM > 9.0 μm); mixed automobiles and coal combustion sources in ST5 (2.1 μm < PM < 3.3 μm); oil combustion, secondary aerosol, and incineration in ST8 (0.4 μm < PM < 0.7 μm); and biomass burning source in ST7 (0.7 μm < PM < 1.1 μm), respectively. The relative contribution of most abundant sources was 32.4% of long-range transport source in the coarse particle mode and 34.5% of secondary aerosol in the fine particle mode, respectively. It seems that the size-resolved analysis by PMF provides useful information on controlling local/regional emission sources and on acquiring scientific knowledge for size-resolved aerosol compositions emitted from specific sources.

Keywords: Cascade impactor; PMF; CPF; Size segregation; Source contribution.

INTRODUCTION

Rapid growth of industrial activities and urban population is a main issue causing serious air pollution problems in Korea. High level of particulate matter (PM) including fine particles affects to reduce visual range, to increase the rate of mortality rate and the number of hospitalization, and especially to increase the perception of air pollution. The PM holds a variety of physical characteristics such as size, shape, density, hygroscopicity, and so on, and chemical characteristics such as contents of heavy metal, water-soluble ingredients, and so on (Hidy, 1972). Among many parameters, the PM size must be closely related to respiratory deposition and visibility. Thus it is considered to be a key parameter in terms of air pollution control and human health/wealth (Appel *et al*., 1985; John *et al*., 1990).

There are numerous aerosol sources including natural and anthropogenic sources in local and regional areas. Various statistical methods like receptor models were playing an important role in identifying those sources. Main purposes for those models are to calculate quantitatively the source contribution at the receptor site and finally to suggest reasonable air pollution control strategies and management policies. However, despite a first study on receptor modeling was introduced about two decades ago (Kim *et al*., 1990) and many studies have been performed in Korea (Kim and Lee 1993, Hwang *et al*., 2001; Hwang *et al*., 2002; Hwang and Kim 2003; Han *et al*., 2006a, b; Shin *et al*., 2006; Kang *et al*., 2008), the local/central government still consider automobile source as a unique and predominant contributor to be controlled and handled. It is because of ignoring scientific basis on the emissions from various sources. Up to the present time, they have estimated only source-oriented PM emissions by summing up all the fuel combustion activities multiplied by simple emission factors and thus failed to notice the emissions from the other man-made sources, natural sources, and secondary sources. Due to the inflation of the

---

[*] Corresponding author. Tel.: 82-031-201-2430;
Fax: 82-031-203-4589
E-mail address: atmos@khu.ac.kr

automobile source contribution for many years in Korea, the government has established blind policies by spending huge budgets to inefficiently control the single source.

Receptor modeling starts from sampling PM, analyzing physicochemical species in the PM, and ends with applying various models to apportioning PM mass. Two receptor models, CMB (chemical mass balance model) and PMF (positive matrix factorization model), have been widely used in many countries. To apply the former model, one needs a priori information on existing emission sources for the study area and further the corresponding source profile obtained by either direct sampling or by literatures. In the urbanized local site like our study area, since there are no source profiles properly designed for receptor modeling, we have applied PMF instead of CMB to reasonably identify local/regional sources.

The purpose of this study is to estimate source contribution to size-resolved PM mass in an urban mixed site in Korea. PM was collected by a cascade impactor and 20 chemical species were analyzed by ICP-AES and IC. In our present study, PMF and CPF (conditional probability function) were intensively used to classify PM sources by checking their direction. Similar previous studies using TTFA (target transformation factor analysis) and PMF had been performed to obtain contributions to TSP, PM_{10}, $PM_{2.5}$ at this sampling site (Kim *et al.*, 1993; Hwang, *et al.*, 2002; Hwang, *et al.*, 2003). However, those apportionment studies were performed by using insufficient numbers of chemical species or applied without size-segregation scheme.

EXPERIMENTAL METHODS

Study Area and Sampling Site

The airborne PM sampling was conducted on the roof of Engineering Building, Kyung Hee University-Global Campus located on the border of two big cities, Suwon City and Yongin City. The two cities are located on the central part of Gyeonggi Province, in the center of the Korean Peninsular. Populations of Yongin and Suwon were 0.86 million and 1.09 million on February 2010, respectively (Suwon City, 2010; Yongin City, 2010). The sampling site (37°14′N, 127°04′E, 20 m above street level) was carefully determined to collect PM samples large enough to minimize the external effect of surrounding barriers or physical environment. A map of Korea showing the location of Suwon and Yongin cities with sampling site is given in Fig. 1.

The two cities are urbanized and mixed with industrial and agricultural areas. There were 181 industrial point sources at the end of 2007 including the Samsung Semiconductor and Samsung Electronics Company, located a few km south from the sampling site (Suwon, 2008). There have been paddy fields inside campus and around the Lake Shingal (52.3 km^2) located on the east. Besides them, there have been distinct local emission sources such as line sources (i.e. 2 major express highways and many local paved roads) and area sources (i.e. fuel combustion for cooking and heating from residential area and fugitive emissions from broad construction areas and from illegal open-burning activities). It was also reported that there were various types of sources affecting the local air quality around the study area (Hwang, 2003).

Meteorological data used in our study were obtained from the nearby Suwon Regional Meteorological observatory. Table 1 shows monthly averaged meteorological parameters during the sampling periods. Main wind directions and average speeds for each season were west in spring and summer; west-northwest in fall, and west-northwest in winter. In addition, it was reported that the Asian dust storms occurred twice in 2005 (Nov. 6, 7), 11 times in 2006 (Mar. 11, 13, 28, Apr.7 till 9, 18, 23 till 24, 30, May. 1),
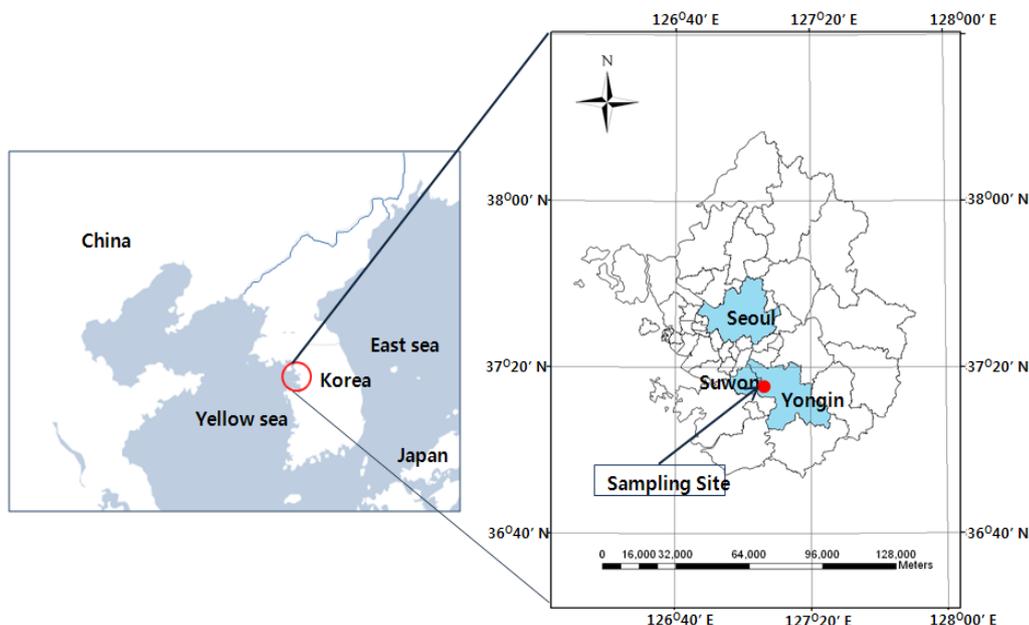

Fig. 1. Map showing two big neighbor cities in Korea with sampling site.

Table 1. Summary of meteorological information during the study period in Suwon (KMA, 2006–2008).

Year	Month	Temp (°C)	R.H. (%)	Prec. (mm)	W.S. (m/s)	W.D.	Sunshine (hr)
2005	Sep.	22.2	71	315.2	2.1	NNE	135.4
	Oct.	14.4	66	70.2	1.3	NW	201.6
	Nov.	8.2	57	38.8	1.5	W	181.6
	Dec.	−3.9	52	12	2.1	NW	197.9
2006	Jan.	−0.4	59	38.6	1.6	WNW	144.8
	Feb.	−0.1	54	19.5	2.1	NW	174.6
	Mar.	5	51	6.9	2.7	SSW	205
	Apr.	11.3	57	59.9	2.7	W	137
	May	18.2	60	133.2	2.2	SSW	197.5
	June	21.7	69	156.7	2	ENE	162.6
	July	23.6	82	754.7	1.9	NE	46
	Aug.	27.5	68	66.4	2.1	ENE	201
	Sep.	21.3	59	21.9	2	ENE	190.2
	Oct.	17.6	67	18	1.6	N	169.9
	Nov.	8.4	58	61.6	2.2	SW	141.8
	Dec.	1.2	60	25.3	1.7	NW	152.5
2007	Jan.	−0.1	65	9.3	1.4	W	178.7
	Feb.	3.3	66	15.1	1.6	WSW	179.2
	Mar.	6	70	135.3	2	WSW	155.3
	Apr.	11.1	64	24.2	2	WSW	211
	May	17.8	69	146.7	1.8	SW	213.2
	June	22.6	69	74.2	1.7	E	185.4
	July	24	82	269.7	1.8	ENE	107.4
	Aug.	26.1	82	295	2.1	ENE	126.3
	Sep.	21.5	81	264.8	1.9	NNE	91.3

Temp.: Temperature
Prec.: Total precipitation
W.D.: Wind direction
R.H.: Relative humidity
W.S.: Wind speed
Sunshine: total sunshine per month

and 10 times in 2007 (Feb. 14, Mar. 6, 27, 28, 31, Apr. 1, May. 8, 9, 25, 26) (KMA, 2006–2008).

Sampling of PM

A low volume 9-stage cascade impactor (Anderson 20-800 series, USA) including back-up stage was employed for size segregated PM sampling at a flow rate of 28.3 L/min. PM was separated into 9 fractions in terms of aerodynamic diameter; > 9 μm on the first stage (ST1), 5.8–9.0 μm (ST2), 4.7–5.8 μm (ST3), 3.3–4.7 μm (ST4), 2.1–3.3 μm (ST5), 1.1–2.1 μm (ST6), 0.7–1.1 μm (ST7), 0.4–0.7 μm (ST8) and < 0.4 μm on the final back-up stage (ST9). Sampling was carried out over 2 years from September 2005 to September 2007 with about 2 weeks integrated sampling to obtain sufficient PM mass required for wet chemical analyses.

PM of each stage was collected on 80 mm membrane filter (Gelman Science Co. Model GN-6, USA) and PM of back-up stage was collected on glass-fiber filter (Adventec Co. Model GB 100R, Japan). The filters right after sampling were put in polyethylene plastic bags and preserved in a refrigerator. All the filters were weighed before and after sampling with an analytical balance (A&D Co., Model HM-202, reading precision of 10 μg) after conditioning at constant temperature and humidity.

PM Extraction and Analytical Methods

A microwave pre-treatment method under Clean Water Act issued by USEPA and a HNO_3-HCl pre-treatment method with Questron's Model Q-15 MicroPrep were used to analyze inorganic elements in PM. To do this, each filter was cut to several pieces with fixed size by a stainless steel cutter, and one of pieces was soaked by HNO_3 (61%) and HCl (35%) solution and heated for 5 minutes. After extraction the solution was filtered by a filter paper (No. 5B, 110 mm, Advantec MFS Inc.), and diluted to 50 mL with deionized water. Each filtrate was analyzed to determine 12 inorganic elements (Al, Mn, V, Cr, Fe, Ni, Cu, Zn, Cd, Ba, Pb, and Si) by inductively coupled plasma atomic emission spectroscopy (ICP-AES, DRE ICP, Leeman Labs Inc., USA). Further a piece of the filter was extracted with ultra pure water and ionic components were ultrasonically extracted. After passing through microporous membrane filters (pore size, 0.45 μm; diameter, 25 mm), each filtrate was used to analyze 5 cations (Na^+, K^+, NH_4^+, Mg^{2+}, and Ca^{2+}) and 3 anions (NO_3^-, SO_4^{2-}, and Cl^-) by ion chromatography (Dionex, Model DX-400), which consists of a separation column (Dionex Ionpac AS12A for anion and CS12 for cation) and a guard column (Dionex Ionpac AG 11 for anion and AG12A for cation).

Prior to use ICP-AES and IC, several standard solutions

with similar level of sample concentration were injected to examine quality assurance. An accuracy check was performed by calculating a relative error (RE) resulting from standard solutions and a precision check was performed by obtaining relative standard deviation and a coefficient of variation (CV) based on 3 repetitive measurements. Table 2 shows RE and CV for each chemical species. REs for Si by ICP-AES and for NH_4^+ by IC were 17.6% and 9.6% in terms of measurement accuracy, respectively. Similarly, CVs for Si by ICP-AES and for NO_3^- by IC were 11.1% and 12.5% in terms of measurement precision, respectively. When analyzing Si, ICP-AES provided relatively low accuracy and precision. Furthermore Zn and Al appeared uniquely at ST9 on which glass-fiber filter was using. It must be because the detection limits of ICP-AES using glass-fiber filter were extremely high for Ba, Zn, and Al. Thus in our PMF modeling, we decided to use the chemical data only obtained at ST1 to ST8 with excluding ST9.

DATA ANALYSIS

The number of sources (or number of factors) statistically determined is highly dependent on number of aerosol samples, number of chemical variables, temporal and spatial variability, various local and regional environments, and study scopes. The number of sources determined by CMB model (used when source profiles are provided or when the number of dominant sources are known) is generally larger number than those by TTFA or PMF model (used when a priori information on source inventory is not provided). However, PMF model is being more practically applied than CMB model since source apportionment results are extremely sensitive to source profiles used or created (Kim *et al.*, 2006; Lee *et al.*, 2007; Lee *et al.*, 2008).

PMF

Factor analysis is used to look for key correlation among measured variables and mainly applied to identify emission sources by interpreting groups of chemical variables with strong correlation. However, when traditional factor analysis depending on covariance matrix is applied, researchers experience physical difficulties due to insufficient information, factor loading of negative value, uncertainty on factor rotation, etc (Hwang, 2001). Such limitations might provide possibilities to bring subjective results when determining a proper number of emission sources and thus they stimulated to develop more improved PMF methodology than traditional factor analysis (Paatero and Tapper, 1994).

PMF analysis always provides positive factor loadings and it depends not only on information of correlation matrix but on the algorithm of least square minimization, namely, on information of error estimation for each data. As all receptor models are keeping the rule of mass balance and mass conservation, so PMF is also expressed as the following mass balance Eq. (1).

$$x_{ij} = \sum_{k=1}^{p} g_{ik} f_{kj} + e_{ij} \tag{1}$$

$$i = 1,2,\ldots, m, \quad j = 1,2,\ldots, n, \quad k = 1,2,\ldots, p$$

where x_{ij} is the ambient concentration of jth chemical species of ith PM sample, g_{ik} is the source contribution of kth source in ith sample, f_{kj} is the source profiles, and e_{ij} is residual error. After the model applies a least squares fitting, Q value expressed in Eq. (2) is used to minimize differences between measured and estimated concentration in PMF modeling. The value is useful to determine the proper number of factors.

$$Q = \sum_{i=1}^{n} \sum_{j=1}^{m} \frac{(x_{ij} - g_{ik} f_{kj})^2}{\sigma_{ij}^2} = \sum_{i=1}^{n} \sum_{j=1}^{m} \left(\frac{e_{ij}}{\sigma_{ij}} \right) \tag{2}$$

where σ_{ij} is the uncertainty of ambient concentration of jth chemical species of ith PM sample. Uncertainty can be flexibly estimated by raw input concentration data based on sampling and analytical environment. This might be an advantage of PMF model compared to the existing factor analysis.

Table 2. Analytical uncertainties of ICP-AES and IC in this study.

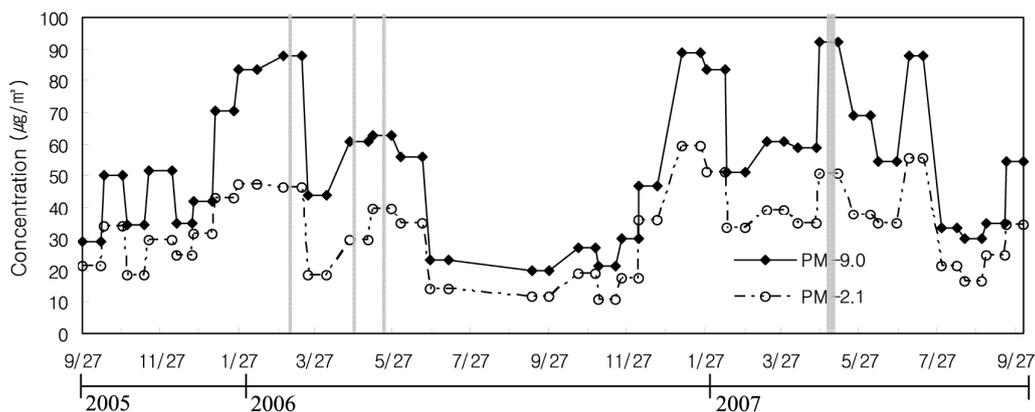| ICP-AES			IC		
Species	RE (%)	CV (%)	Species	RE (%)	CV (%)
Ba	2.25	1.26	Na^+	-1.69	1.07
Fe	0.3	1.12	NH_4^+	9.55	0.23
Al	−1	2.13	K^+	1.2	1.98
Si	17.63	11.08	Mg^{2+}	2.42	0.89
Mn	−0.43	1.06	Ca^{2+}	3.29	2.72
Ni	0.43	3.09	Cl^-	−4.99	2.57
Cu	−2	3.07	NO_3^-	−1.69	12.54
Cd	1.25	1.9	SO_4^{2-}	−4.46	5.48
V	1	0.75			
Pb	0.5	6.15			
Cr	2.25	1.26			
Zn	1.5	1.23			

Input Data

A total of 32 sets of PM data were obtained from a 9-stage cascade impactor that had been consecutively operated for approximately 2 years. Backup stage (ST9) was excluded for PMF analysis. Two-year average concentration of each chemical species for each size range is shown in Table 3.

Major inorganic species for all size ranges were Fe, Al, Si, Zn, Ni, and Pb. Concentrations of Fe, Al, Si, Mn were much higher in the coarse fraction, while those of Ni, Cu, Cd, V, Pb, Cr, Zn were much higher in the fine fraction. The former must be mainly influenced by crustal sources and the latter must be mainly emitted by man-made sources. Fig. 2 shows

Table 3. Average concentrations of PM mass (µg/m^3), inorganic elements (ng/m^3), and ionic components (ng/m^3) for each size range during the study period of September 2005 to September 2007.

| Size (µm) | Stage | | | | | | | | Fine 0.4 < PM < 2.1 | Coarse > 2.1 | Total |
	ST8 0.4–0.7	ST7 0.7–1.1	ST6 1.1–2.1	ST5 2.1–3.3	ST4 3.3–4.7	ST3 4.7–5.8	ST2 5.8–9.0	ST1 >9.0			
PM[a]	9.3	9.2	6.5	5	6	3.3	6.3	11.7	25	32.3	57.3
	± 3.9	± 6.1	± 3.5	± 2.8	± 2.8	± 1.8	± 3.5	± 8.2	± 3.5	± 19.1	± 22.6
Ba	2.2	2.8	5.3	5.4	5.4	3.1	4.9	5.3	10.3	24.1	34.4
	1.2	± 2.1	± 2.1	± 2.2	± 2.2	± 1.6	± 1.9	± 2.5	± 5.4	± 10.4	± 15.8
Fe	73.7	45.8	81.1	118.3	111.4	62.1	131.8	181.8	200.6	605.4	806
	± 64.2	± 42.4	± 64.6	± 94.9	± 82.3	± 43.8	± 101.7	± 134.6	± 171.2	± 457.3	± 628.5
Al	46.4	43.6	54.3	60.4	62.4	52.5	85	104.7	144.3	365	509.3
	± 26.0	± 33.8	± 40.3	± 55.4	± 60.1	± 43.2	± 62.5	± 64.6	± 100.1	± 285.8	± 385.9
Si	20.8	29.2	43.1	46.2	67.7	42.7	71.1	79.9	93.1	307.6	400.7
	± 24.9	± 33.2	± 31.9	± 31.0	± 35.7	± 34.0	± 47.3	± 40.0	± 90.0	± 188.0	± 278.0
Mn	3.5	4.2	4	3.1	4.8	3.4	4.5	5.8	11.7	21.6	33.3
	± 2.1	± 2.7	± 2.2	± 2.0	± 6.4	± 6.4	± 3.7	± 5.1	± 7.0	± 23.6	± 30.6
Ni	16.8	12.7	13.8	14.3	12	14	15.5	14.9	43.3	70.7	114
	± 14.0	± 8.9	± 10.9	± 13.9	± 8.8	± 12.7	± 13.5	± 11.6	± 33.8	± 60.5	± 94.3
Cu	9	9.3	12	10.4	m8.7	11.6	11.3	10	30.3	52	82.3
	± 8.7	± 7.5	± 9.4	± 9.0	± 9.0	± 8.6	± 8.5	± 8.9	± 25.6	± 44.0	± 69.6
Cd	1.7	1.8	1.8	1.6	1.7	1.5	1.4	1.5	5.3	7.7	13
	± 1.4	± 1.3	± 1.4	± 1.3	± 1.5	± 1.3	± 1.4	± 1.5	± 4.1	± 7.0	± 11.1
V	2.3	1.5	2.6	2.2	2.8	1.9	2.2	1.8	6.4	10.9	17.3
	± 1.7	± 1.2	± 2.6	± 1.4	± 1.5	± 1.5	± 1.1	± 1.6	± 5.5	± 7.1	± 12.6
Pb	16.2	20.9	19.1	15.6	20.7	19	12.5	12.5	56.2	80.3	136.5
	± 15.8	± 16.7	± 17.0	± 14.2	± 22.1	± 17.4	± 9.8	± 12.2	± 49.5	± 75.7	± 125.2
Cr	5.3	5.8	6.6	13.6	7.2	5	5.3	9	17.7	40.1	57.8
	± 4.9	± 4.8	± 5.8	± 16.6	± 6.5	± 3.5	± 6.7	± 9.7	± 15.5	± 43.0	± 58.5
Zn	13.8	18.9	18.5	8.3	5.6	3.4	5.2	8.3	51.2	30.8	82
	± 10.5	± 13.5	± 14.1	± 8.6	± 5.8	± 4.0	± 3.9	± 4.5	± 38.1	± 26.8	± 64.9
Na$^+$	132.2	154.3	154.6	168	153.1	124.8	158.8	186.9	441.1	791.6	1,232.70
	± 131.6	± 127.1	± 114.1	± 113.0	± 73.7	± 89.5	± 109.4	± 170.1	± 372.8	± 555.7	± 928.5
NH$_4^+$	888.5	877.6	374.6	113.6	74.6	71.1	84	108.6	2,140.70	451.9	2,592.60
	± 335.6	± 451.1	± 285.4	± 64.0	± 41.9	± 34.2	± 39.9	± 46.0	± 1,072.1	± 226.0	± 1,298.1
K$^+$	112.1	144.7	51.1	29.8	23.6	27.8	37.5	35.6	307.9	154.3	462.2
	± 85.6	± 118.1	± 33.2	± 22.6	± 15.4	± 31.6	± 70.8	± 20.6	± 236.9	± 161.0	± 397.9
Mg^{2+}	87.1	106.5	86.3	82.8	80.6	70.5	77.9	94.1	279.9	405.9	685.8
	± 64.2	± 59.7	± 44.8	± 37.5	± 43.3	± 39.0	± 40.7	± 48.7	± 168.7	± 209.2	± 377.9
Ca^{2+}	217.3	244	217	222.2	201.5	185.8	246.8	347.2	678.3	1,203.50	1,881.80
	± 148.1	± 140.8	± 149.5	± 94.8	± 111.1	± 93.8	± 133.4	± 212.0	± 438.4	± 645.1	± 1,083.5
Cl$^-$	279.9	236.7	161.2	135.7	99.9	69.4	128.4	178.1	677.8	611.5	1,289.30
	± 225.5	± 208.4	± 121.4	± 80.5	± 65.4	± 53.6	± 76.3	± 121.9	± 555.3	± 397.7	± 953.0
NO$_3^-$	1,441.20	1,466.30	939.6	549.2	516.9	295.9	430.2	608.1	3,847.10	2,400.30	6,247.40
	± 803.3	± 1,000.6	± 586.4	± 363.2	± 273.7	± 158.9	± 205.4	± 316.0	± 2,390.3	± 1,317.2	± 3,707.5
SO$_4^{2-}$	2,120.10	2,166.10	977.4	323.5	178	95.3	210.6	288	5,263.60	1,095.40	6,359.00
	± 936.0	± 1,227.6	± 714.1	± 213.2	± 72.3	± 51.4	± 106.3	± 178.0	± 2,877.7	± 621.2	± 3,498.9

[a] Unit: µg/m^3

Fig. 2. Temporal variation of PM-9.0 and PM-2.1 concentrations observed from September 2005 to September 2007 at the sampling site.

the variation of PM-2.1 and PM-9.0 concentration during the sampling period. The temporal patterns of PM-2.1 and PM-9.0 were quite similar each other. The levels were generally high in winter and low in summer. Some of high peaks appeared during the Asian dust storm episodes, which were in the plot with shadow areas.

Data Treatment and PMF Modeiling

A total of 8 input data sets, consisting of 20 chemical variables and 32 samples for 8 size ranges, were prepared for PMF. PMF modeling was separately performed for each size range. In our study, Q-mode analysis was applied to obtain a matrix of correlations among samples by arranging the samples in rows and chemical variables in columns on each data sheet.

When there are incomplete data sets containing data below detection limit or missing data, there are several methods to substitute by approximated values. In this study, values below detection limit were substituted by the half value of detection limit and missing values are substituted by the geometric average of relevant chemical species described in the previous reports (Polissar *et al.*, 1998; Lee *et al.*, 2002). As a matter of fact, PMF model requires a pair of data for each variable consisting of a measured value plus a corresponding uncertainty. It was reported that the uncertainty, u_{ij}, could be calculated like the following Eq. (3) (Polissar *et al.*, 1998).

$$u_{ij} = [DL]/3 + h \times x_{ij} \qquad (3)$$

where u_{ij} is the uncertainty of jth chemical species of ith sample, x_{ij} is the ambient concentration of jth chemical species of ith sample, h is the fractional error, and DL is the detection limit. The h can be presumed by linear relationship between the two values of measured concentration and analytical uncertainty (Kim *et al.*, 2005). Thus, uncertainty for each variable was approximated by the above Eq. (3).

In any factor analysis, one of important steps is to choose proper number of factors. The optimum number of factors can be determined by trial and error (Song *et al.*, 2001). A method to find out the number is using Q value described in

Eq. (2). This step minimizes the difference between true measured value and theoretical value. Then the theoretical Q values should be equal to the values subtracting all elements in a factor matrix from data matrix and further standardized residuals in residual matrix ***R*** should be within –2.0 and +2.0 with the probability of 0.8 (Hopke 2000; Ramadan *et al.*, 2000; Polissar *et al.*, 2001). In addition, the maximum individual column mean (called IM in PMF model) and standard deviation (called IS in PMF model) can be calculated from the matrix ***R*** to determine proper factors. Generally IM and IS remarkably decrease as Q decreases (Lee *et al.*, 1999). In our study, IM and IS were examined for each relevant number of factors. Details were described in the previous paper (Oh *et al.*, 2009).

As results given in Table 4, 4 to 6 factors were determined for each of 8 size-segregated data sets. After choosing the number of factors, modeling was conducted by repeatedly increasing 0.1 of ***Fpeak*** between –1.0 and 1.0. The rotational matrix (called ***Rotmat***) explaining uncertainty of factor rotation is used as a criterion by determining degree of freedom. The largest element in ***Rotmat*** indicated maximum uncertainty of rotation at the corresponding ***Fpeak*** value (Lee *et al.*, 1999). Generally optimum degree of rotational freedom can be determined with preserving a certain limit of Q values (Song *et al.*, 2001; Kim *et al.*, 2003; Han *et al.*, 2006). Optimum modeling conditions for ***Fpeak*** and Q value used in our study are given in Table 4.

Conditional Probability Function

Conditional probability function (CPF) was used to examine the relationship of source contributions with wind direction described in Kim and Hopke (2004a). To estimate the potential location of identified sources after PMF modeling, the CPF described in Ashbaugh *et al.* (1985) and Kim *et al.* (2004b) was extensively applied. The technique estimates the probability that a given source contribution from a given wind direction exceeds a given threshold concentration. CPF can be mathematically expressed as the following Eq. (4).

$$CPF_{\Delta\theta} = \frac{m_{\Delta\theta}}{n_{\Delta\theta}} \qquad (4)$$

Table 4. Optimum PMF modeling conditions for each stage.

Modeling parameter	ST1	ST2	ST3	ST4	ST5	ST6	ST7	ST8
Number of factors	4	4	5	5	5	5	6	5
Robust mode (a)	4	4	4	4	4	4	4	4
Fpeak	–0.4	–1	–0.1	–0.5	–0.2	–0.2	0	–0.9
Q value	380.2	370.9	241.7	316	328.2	376.2	280.9	334
Scales residual (%)	97.5	97.8	98.7	96.7	98.3	97.7	97.7	97.5

where $m_{\Delta\theta}$ is the number of times air parcels from the wind sector $\Delta\theta$ exceeded a given criterion and $n_{\Delta\theta}$ is the total number of data points from the wind sector $\Delta\theta$. Identified sources are then potentially located in the directions which have high CPF values (Kim and Hopke, 2004c, d).

As reported in the previous study (Guerra *et al.*, 2006), wind direction surely contributes to temporal variation in air pollutants emitted from specific sources. In our study, we calculated probabilities that PM concentrations coming from 16 sectors of wind direction divided by 22.5° per sector exceeded average values. After exploring several levels of threshold criteria, we decided to use the upper 20th percentile for the fractional contribution from each source. Calm wind conditions with wind speed less than 1 m/sec were excluded in our analysis.

RESULTS AND DISCUSSION

Size Segregated and Profile

As shown in Table 4, the number of factors at each size range were determined as follows; four factors at ST1, ST2, five factors at ST3, ST4, ST5, ST6, ST8, and six factors at ST7, respectively. According to various information such as mass fraction of chemical species, ratio among specific species, pattern of time series, and reference source profiles, each statistical factor by PMF can be restored as an emission source that is physically interpretable in the real world.

A total of 39 source profiles were initially prepared since each of 8 stages provided 4 to 6 sources. However, only 11 sources were finally determined in this study because many sources at one stage were repeatedly duplicated at other stages as shown in Table 5. For example, the oil combustion source designated as one of 11 sources

appeared 6 times at ST3 to ST8 (0.4 μm < PM< 5.8 μm) and both long-ranged transport and soil sources appeared 5 times at ST1 to ST5 (PM > 2.1 μm). The sources such as sea salt, road dust, soil, long-ranged transport, and NH_4NO_3 related sources dominantly appeared from ST1 to ST5 where coarse particles larger than 2.1 μm were collected. On the other hands, the sources such as coal combustion, incineration, and biomass burning sources appeared from ST5 to ST8 where fine particles smaller than 2.1 μm were collected. In case of mixed automobile source, it appeared at ST3 to ST7 with the size range of 0.7 to 5.8 μm.

The repetition of sources consecutively appearing at next size ranges provided useful information when classifying undefined sources into potential sources. Thus an obscure source at a certain stage if any could be easily determined by examining temporal patterns of contribution at neighbor stages. As a matter of fact, sources can be misclassified when construction of source inventory (or source library) is poor, when numbers of measured fingerprint variables are not enough to trace sources, or when many complex sources exist. Despite only 4 to 6 sources were obtained at each stage, the results of contribution produce affluent information to control a specific emission source in local area, to assess their impacts on health and wealth, and to study size-segregated aerosol compositions from specific sources.

Size-resolved source profiles and their corresponding temporal contributions are shown in Figs. 3 to 13. The time series distributions were plotted by about 2 weeks contributions to PM mass concentrations in each size-range. Conditional probabilities of potential source directions for 11 sources are plotted in Fig. 14.

Table 5. Sources identified in each size range.

Source	Marker species	ST1	ST2	ST3	ST4	ST5	ST6	ST7	ST8
Aged sea salt	Na^+, Cl^-, Mg^{2+}, Ca^{2+}, SO_4^{2-}, NO_3^-	+	+						
Construction debris	SO_4^{2-}, NO_3^-, Ca^{2+}, Mg^{2+}, Na^+, Cl^-, Si	+	+						
Long-range transport	NO_3^-, SO_4^{2-}, NH_4^+, Fe, Si, Ca^{2+}, Cl^-	+	+	+	+	+			
Soil and road dust	Si, Al, Fe, Cl^-, NO_3^-, SO_4^{2}	+	+	+	+	+			
NH_4NO_3 related	NO_3^-, NH_4^+, Si, Fe^+, Na^+, SO_4^{2-}			+	+				
Oil combustion	SO_4^{2-}, NO_3^-, Na^+, Ca^{2+}, Fe, Si, Ni, V			+	+	+	+	+	+
Mixed automobiles	SO_4^{2-}, NO_3^-, Ca^{2+}, Na^+, Fe			+	+	+	+	+	
Coal combustion	NO_3^-, SO_4^{2-}, NH_4^+, Fe, Si, Cu					+	+	+	+
Secondary aerosol	SO_4^{2-}, NO_3^-, NH_4						+	+	+
Incineration	NO_3^-, SO_4^{2-}, Cl^-, NH_4^+, Fe, Zn, Si						+	+	+
Biomass burning	SO_4^{2-}, NO_3^-, NH_4^+, K^+, Ca^{2+}, Na^+							+	+

Size Segregated Source Profile

As the first factor, aged sea salt source was identified at ST1 and ST2 (PM > 5.8 μm). Fig. 3(a) shows the source profiles separately determined at ST1 and ST2 and Fig. 3(b) shows the time series of contribution at the corresponding stage. The temporal patterns on the figure show almost same shapes with different strengths. The sea salt is well known coarse particles naturally generated from the Yellow Sea (or called Hwanghae), which is lying between the Korean peninsula on the east and China on the west and north. It is about 700 km wide on an average from east to west. Since the sea derived its name from the color of the silt-laden water discharged from the major Chinese rivers (http://www.britannica.com/EBchecked/topic/65268 6/Yellow-Sea), some of crustal species are deservedly expected in this source. Marker species of natural sea salt source were reported as Na^+, Cl^-, SO_4^{2-}, Mg^{2+}, K^+, and Ca^{2+} by (U.S. EPA, 1999). It was reported that Na^+ and Cl^- had a fraction of more than 30 percent and Mg^{2+}, K^+, and Ca^{2+} had a fraction of more than 1 percent in a sea salt source (Lewis and Schwartz, 2004).

The source in this study was characterized by Na^+, Cl^-, Mg^{2+}, Ca^{2+} and the concentrations of Mg^{2+} and Ca^{2+} were especially high as expected. It was also reported that some of NO_3^- existed in aged sea salt as a form of $NaNO_3$ in the coarse fraction (Jonson *et al.*, 2000; Anlauf *et al.*, 2006). Fig. 14(a) shows a CPF plot for the aged sea salt source demonstrated well its location of the Yellow Sea.

The second factor was characterized by SO_4^{2-}, NO_3^-, Ca^{2+}, Mg^{2+}, Na^+, Cl^-, Si, and it appeared at ST1 and ST2 (PM > 5.8 μm) in the coarse fraction as shown in Fig 4(a).
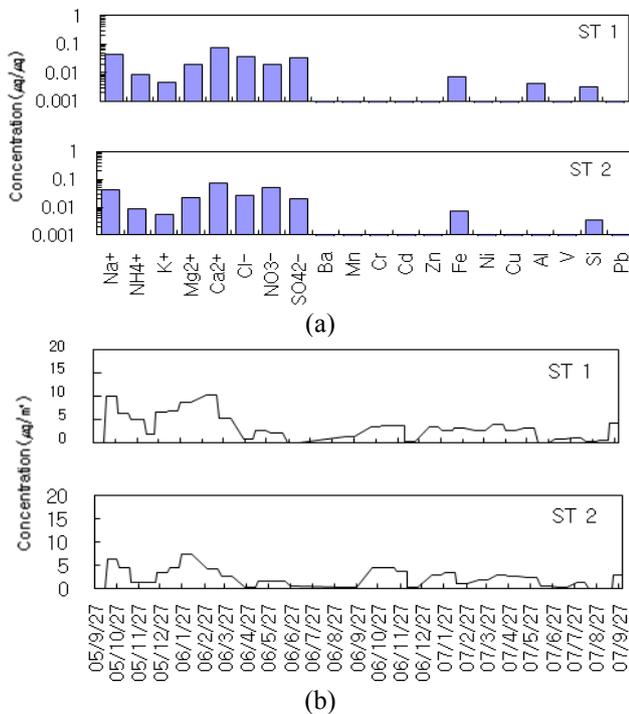
According to a temporal pattern of contribution in Fig. 4(b), it was considered as the construction debris source nearby sampling site since the pattern of source strength agreed well with the remodeling periods of the Engineering Building. The CPF plot for the source in Fig. 14(b) demonstrated direction of the remodeling source located east from the monitoring site. The source contribution to total mass concentration was very small less than a single percent.

The third factor was identified as long-range transport source mostly laden the Asian dust (or called Yellow Sand or Hwangsa). The source appeared at ST1 thru ST5 (> 2.1 μm) in the coarse fraction as shown in Table 6. In Fig. 5(a), the source was dominated by NO_3^-, SO_4^{2-}, NH_4^+, Fe, Si, Ca^{2+}, Cl^- in order. It seemed that various sources such as soil, secondary aerosol, and industrial sources were well mixed during long-range transport from the source origin (Mori *et al.*, 2003; Takahashi *et al.*, 2010). The 5 plots in Fig. 5(b) show temporal patterns of its contributions from ST1 to ST5. The strength of the contribution gradually decreases as particle size decreases. As the size decreases, many water-soluble ions appear and their concentrations increase based on the source profiles. There are distinguished peaks on April and May of 2006 in the temporal contribution plots. As a matter of factor, the Asian dust storms were reported on April and May 2006. Thus the source contribution was considerable during the springtime. According to the size-resolved profiles in Fig. 5(a), Na^+ and K^+ were not observed at ST1 and ST2 (> 5.8 μm), but they appeared at ST3, ST4, and ST5 (2.1 μm < PM < 5.8 μm). However, NO_3^-, SO_4^{2-}, and NH_4^+ were steadily observed at ST1 thru ST5 in this source. The CPF plot in Fig. 14(c) demonstrates its potential

Fig. 3. (a) Aged sea salt source profiles obtained at ST1 and ST2, respectively. (b) Time series of corresponding contributions by PMF model.
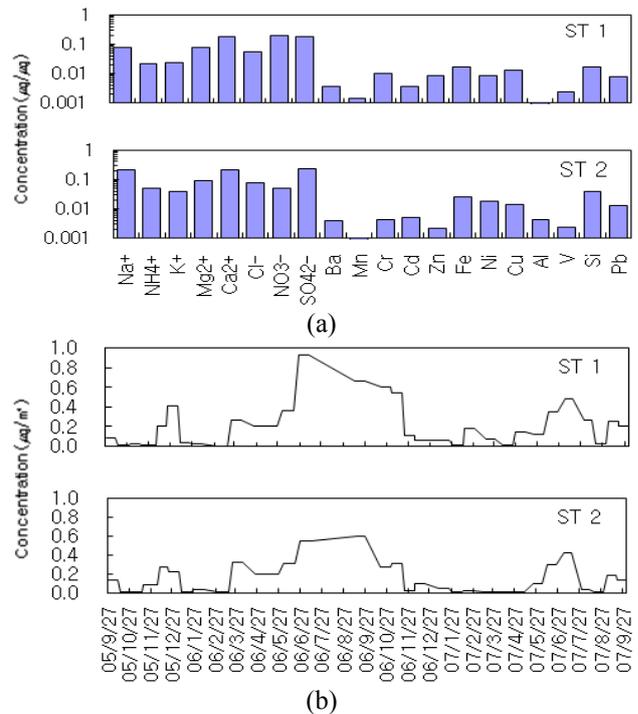
Fig. 4. (a) Construction debris source profiles obtained at ST1 and ST2, respectively. (b) Time series of corresponding contributions by PMF model.

Table 6. Average source contributions (μg/m^3) to size segregated mass concentrations from Sep. 2005 to Sep. 2007.

Stage (Size, μm)	Aged sea salt	Construction debris	Long-range transport	Soil and road dust	NH$_4$NO$_3$ related	Oil Combustion	Mixed automobiles	Coal combustion	Secondary aerosol	Incineration	Biomass burning	Total
ST1 (> 9.0)	3.41 (6.2)	0.22 (0.4)	5.37 (9.8)	2.71 (4.9)	–	–	–	–	–	–	–	11.71 (21.3)
ST2 (5.8–9.0)	2.36 (4.3)	0.15 (0.3)	2.91 (5.3)	0.69 (1.3)	–	–	–	–	–	–	–	6.11 (11.1)
ST3 (4.7–5.8)	–	–	0.32 (0.6)	0.30 (0.5)	0.86 (1.6)	0.08 (0.1)	1.60 (2.9)	–	–	–	–	3.16 (5.8)
ST4 (3.3–4.7)			0.84 (1.5)	0.68 (1.2)	1.92 (3.5)	0.11 (0.2)	1.90 (3.5)	–	–	–	–	5.45 (9.9)
ST5 (2.1–3.3)			0.84 (1.5)	0.20 (0.4)	–	0.17 (0.3)	2.37 (4.3)	1.73 (3.2)	–	–	–	5.31 (9.7)
ST6 (1.1–2.1)			–	–	–	0.30 (0.5)	1.04 (1.9)	1.70 (3.1)	1.61 (2.9)	1.61 (2.9)	–	6.26 (11.4)
ST7 (0.7–1.1)			–	–	–	0.30 (0.5)	0.89 (1.6)	1.24 (2.3)	3.17 (5.8)	0.71 (1.3)	1.82 (3.3)	8.13 (14.8)
ST8 (0.4–0.7)			–	–	–	0.61 (1.1)	–	1.53 (2.8)	3.21 (5.9)	2.60 (4.7)	0.79 (1.4)	8.74 (15.9)
Coarse (PM > 2.1)	5.77 (18.2%)	0.37 (1.2%)	10.28 (32.4%)	4.58 (14.4%)	2.78 (8.8%)	0.36 (1.1%)	5.87 (18.5%)	1.73 (5.5%)	–	–	–	31.74 (100%)
Fine (0.4 < PM < 2.1)	–	–	–	–	–	1.21 (5.2%)	1.93 (8.3%)	4.47 (19.3%)	7.99 (34.5%)	4.92 (21.3%)	2.61 (11.3%)	23.13 (100%)
Total	5.77 (10.5%)	0.37 (0.7%)	10.28 (18.7%)	4.58 (8.3%)	2.78 (5.1%)	1.57 (2.9%)	7.80 (14.2%)	6.20 (11.3%)	7.99 (14.6%)	4.92 (9.0%)	2.61 (4.8%)	54.87 (100%)
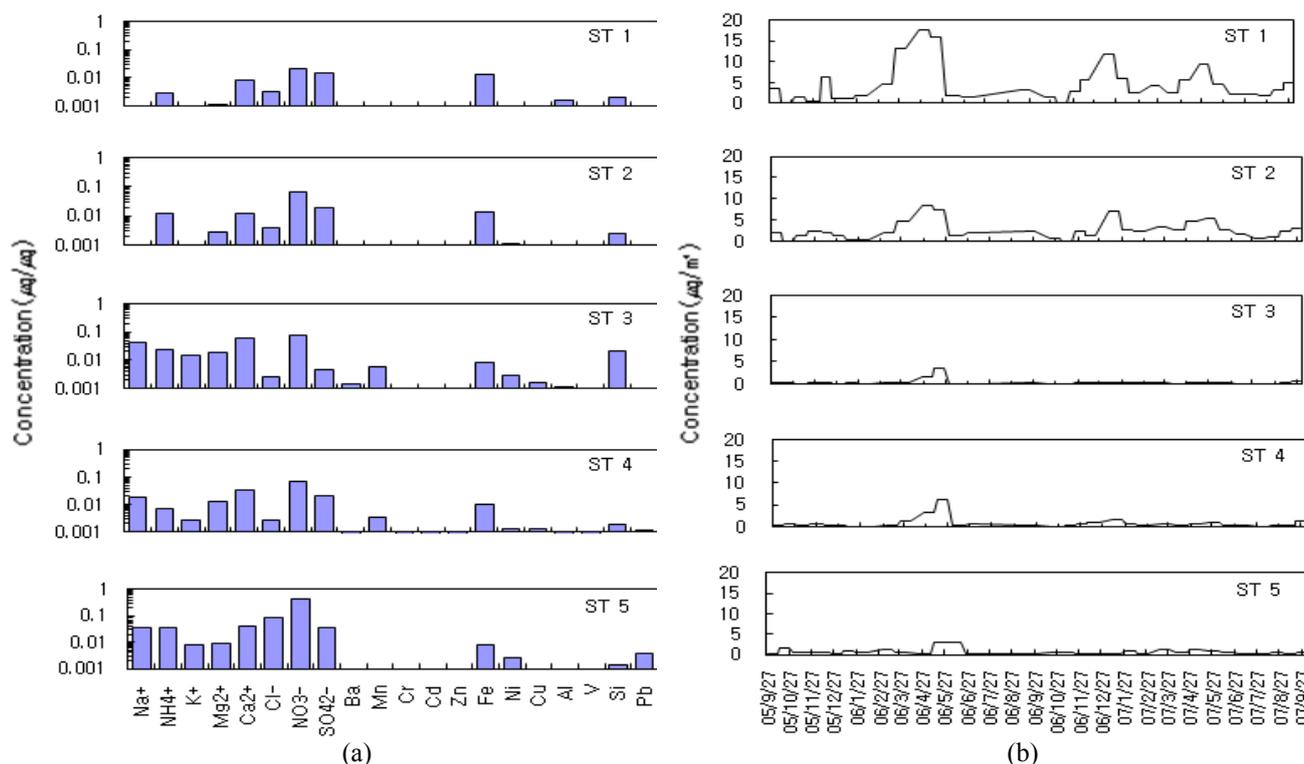
Fig. 5. (a) Long range transport source profiles obtained at ST1 to ST5, respectively. (b) Time series of corresponding contributions by PMF model.

direction of the regional source located southwest from the monitoring site, even though CPF analysis has a limit when identifying long-range transport sources.

The fourth soil and road dust source was characterized by Al, Fe, Si, Cl$^-$, NO$_3^-$, SO$_4^{2-}$, Ca^{2+} as shown in Fig. 6(a) The source appeared at ST1 to ST5 (> 2.1 μm) in the coarse fraction. It was reported that Si had a fraction of more than 10 percent in a typical soil source for coarse

particles (Chow, 1995). However, the fractions of both Al and Fe were slightly higher than that of Si on the average in this study. It seems that high analytical uncertainty of Si by ICP-AES may cause those differences. In Fig. 6(b), the patterns of temporal distribution at ST1, ST2, ST4 were somewhat different from those at ST3 and ST5. This source contribution to mass concentrations at ST3 and ST5 was much smaller than that at ST1, ST2, ST4 as presented in Table 6. The CPF plot in Fig. 14(d) pointed two distinct directions such as southwest and northeast. Huge soil digging works for building apartment complexes had been continued about 500 m southwest as well as about 2 km northeast from the sampling site. Two different source locations might be causing two different temporal distribution in Fig. 6(b). In addition, it seemed probable that some materials such Cl^- and Ca^{2+} as snow-melting agent sprayed in winter were resuspended into the air. Thus this source can be interpreted as the mixed source of typical soil and resuspended road dust in local area.

NH_4NO_3 related source was identified as the fifth factor. This source appeared at ST3 and ST4 (3.3 μm < PM < 5.8 μm) in the coarse fraction. As shown in Fig. 7(a), NO_3^-, NH_4^+, Si, Fe, Na^+, SO_4^{2-} were dominant in order. NO_3^- is generally produced in polluted urban areas from various combustion activities and it is also a well known compound found in the fine fraction. However NO_3^- in this source was dominant in the coarse fraction. In our previous study (Oh *et al.*, 2009) and from Table 4, distinct bimodal distribution was observed for both NO_3^- and NH_4^+, with a small peak at ST3 in coarse fraction and a big peak ST7 in fine fraction. Likewise two peaks were also observed for Si,

Fe, and Na^+, but with a big peak at ST3 in coarse fraction and a small peak at ST7 in fine fraction. In the other study of frequency distribution in various particle sizes in southern California (John *et al.*, 1990), three clear peaks were observed for NO_3^-, NH_4^+, and SO_4^{2-} with two peaks in fine fraction and one in coarse fraction. The presence of nitrate in larger particles characterized by crustal material can be due to the reaction of gas-phase nitric acid with mineral dust (Feng *et al*, 2007; Hwang *et al*, 2006). It seemed that this coarse NH_4NO_3 related source was associated with emissions from agricultural activities near sampling site. There had been cultivating activities in campus paddy field located southeast and additional soil works converting huge paddy field into apartment complexes located about 500 m southwest from the site. These activities agreed well with source direction shown on a CPF plot in Fig. 14(e).

The species of SO_4^{2-}, NO_3^-, Na^+, Ca^{2+}, Fe, Si, Ni, V indicated various types of oil combustion as the sixth factor. This source was observed over many size ranges from ST3 to ST8 (4.7 μm < PM < 0.4 μm). In general, Ni and V are well-known marker elements of oil combustion in the fine fraction (Hopke, 1985; Chow, 1995; Song *et al*., 2001; Lee *et al*., 2002; Morawska and Zhang, 2002). Such markers are mainly emitted from diesel oil or residual oil combustion and the other markers like Na, Ca, NO_3^-, SO_4^{2-} are also released by burning processes using various liquid oils (Hopke, 1985; Schroeder and Dockery, 1987; Chow, 1995). Also Fe is an affluent maker element in oil emissions. The 6 plots in Fig. 8(b) showed a series of temporal contributions obtained from ST3 to ST8. The

(a)   (b)
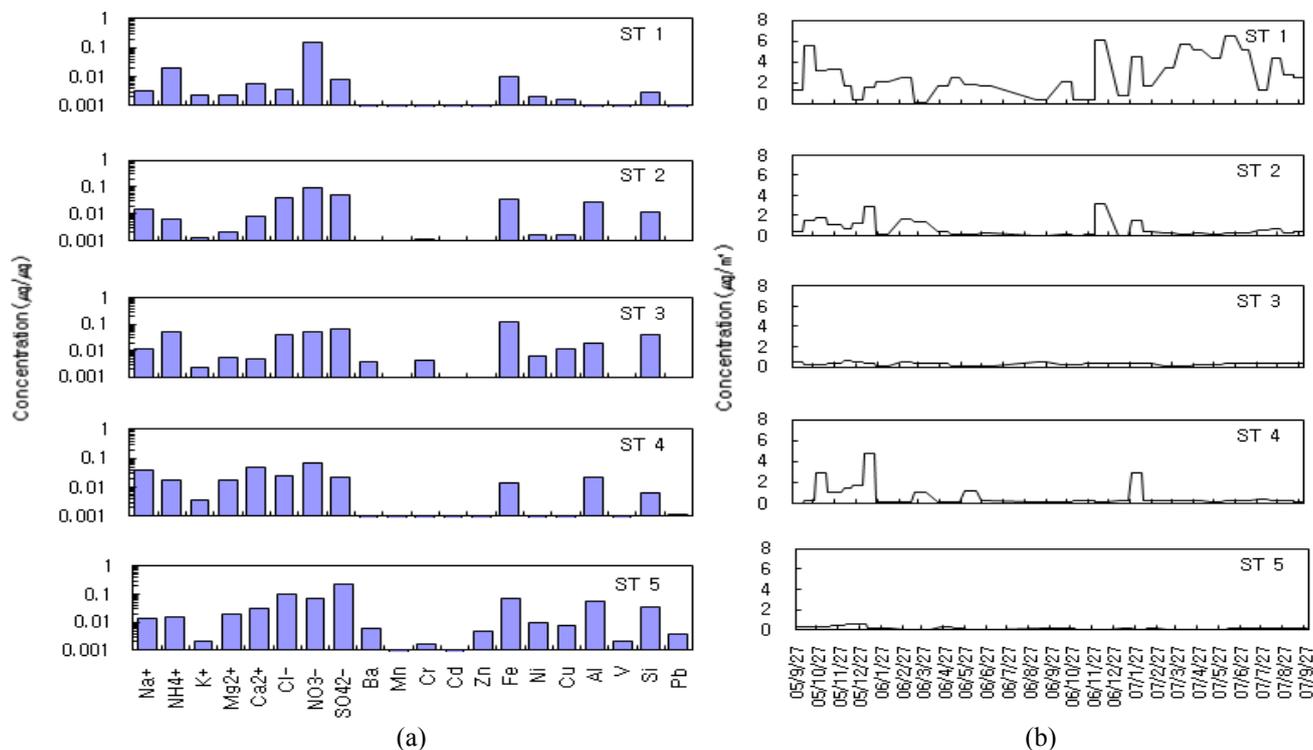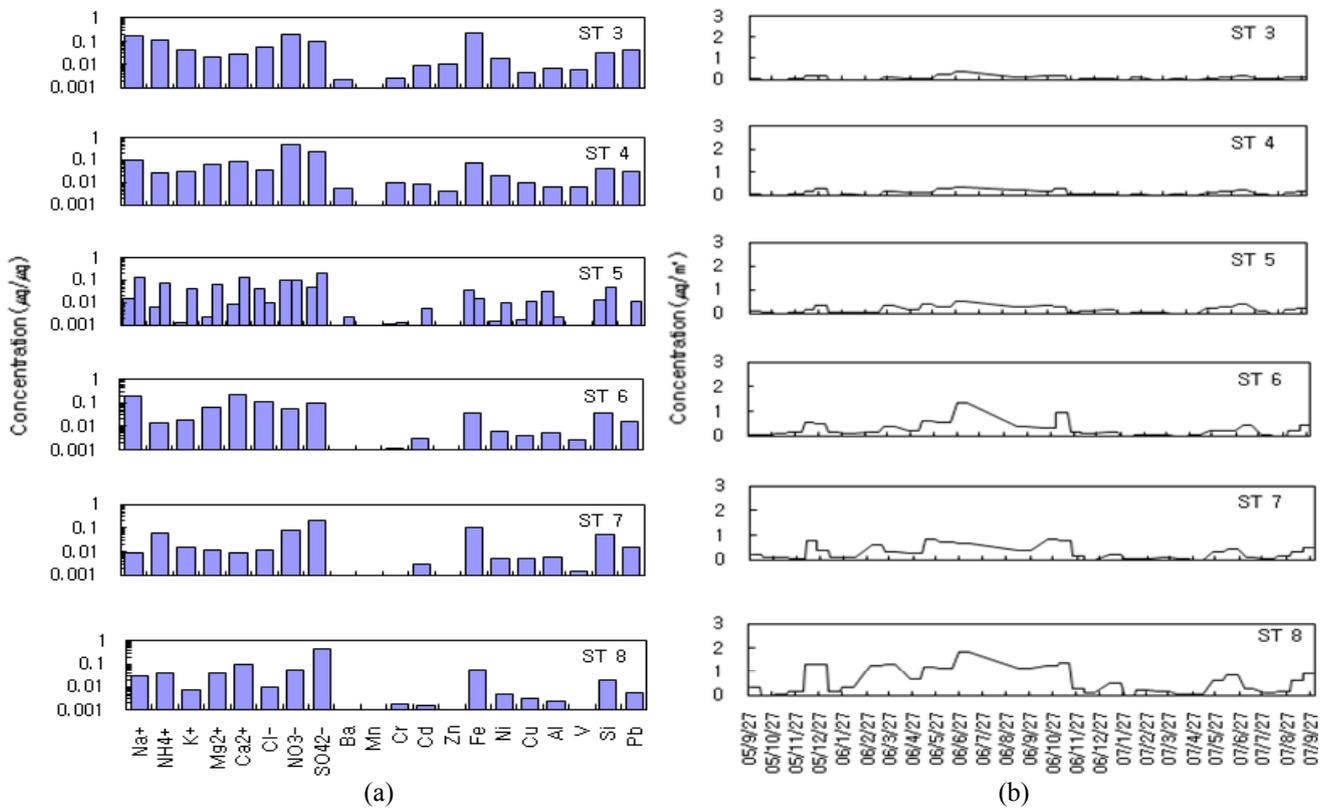
Fig. 6. (a) Soil and road dust source profiles obtained at ST1 to ST5, respectively. (b) Time series of corresponding contributions by PMF model.
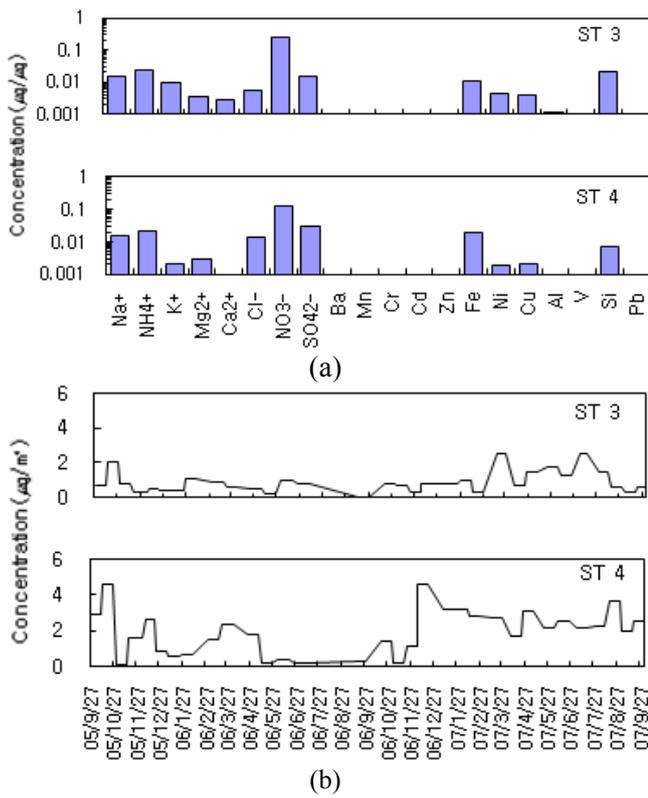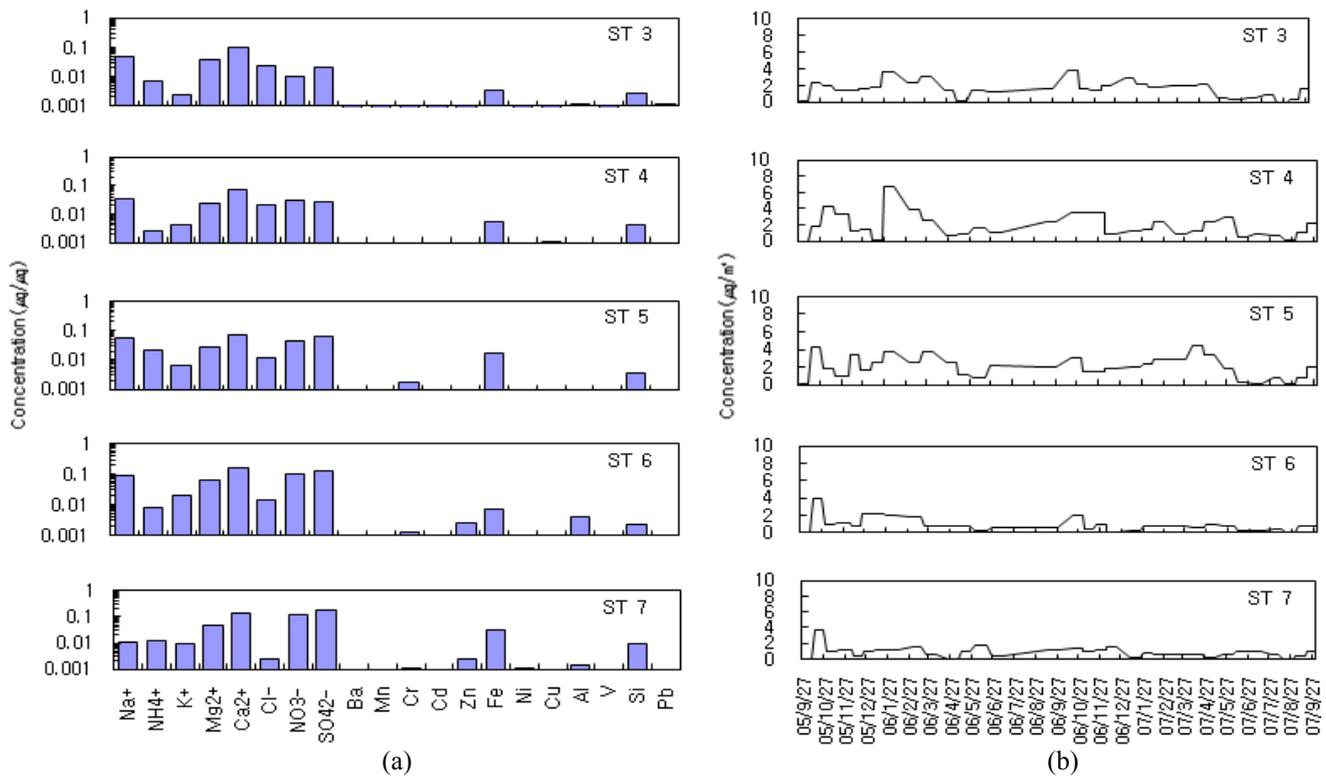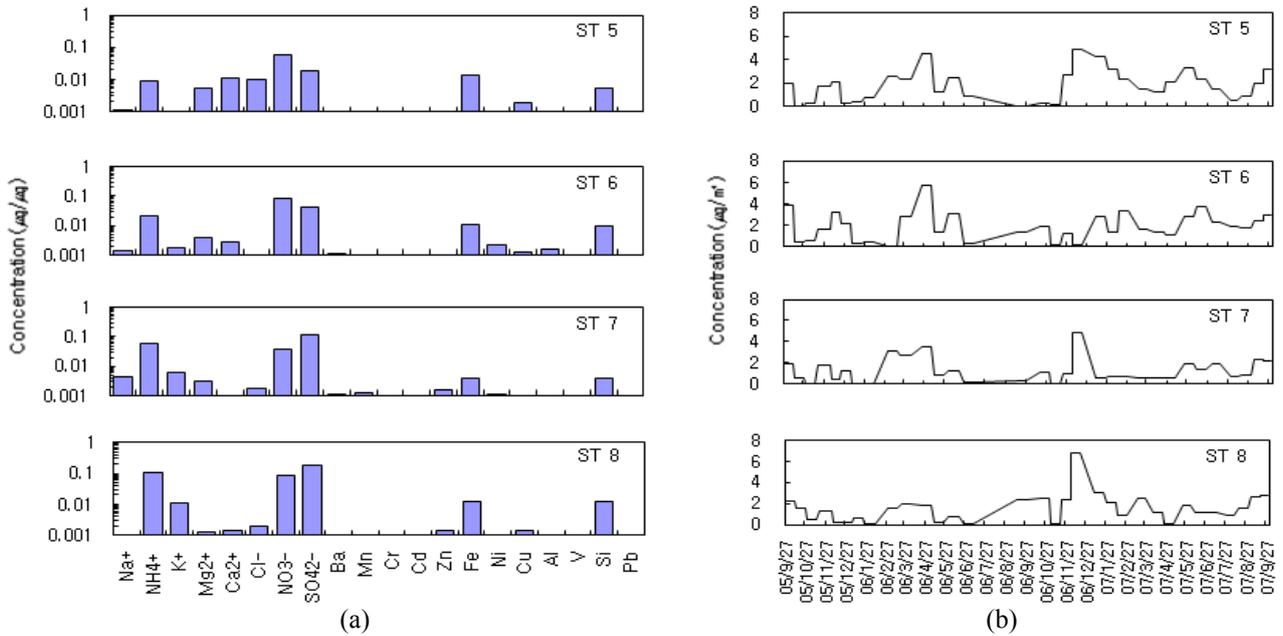
Fig. 7. (a) NH₄NO₃ related source profiles obtained at ST3 and ST4, respectively. (b) Time series of corresponding contributions by PMF model.

strength of the contribution is gradually increasing as particle size decreases. Even though there are many oil combustion sources near the study area, the overall contribution of the source has been decreased because many industries have quickly replaced energy supply systems using liquid fuels into electricity or gaseous fuels according to a government regulation of preventing high sulfur B-C oil in urban area. The CPF plot in Fig. 14(f) showed direction of this local source located north to northeast, where many scattered small-scale industries using various oil fuels are located.

As the seventh factor, mixed automobile source was determined by SO_4^{2-}, NO_3^-, Ca^{2+}, Na^+, Fe, Zn, Si at ST3 to ST7 (0.7 μm < PM < 5.8 μm). Unfortunately Pb as a marker element was not involved in this source. It was observed that Ca^{2+} together with SO_4^{2-} and NO_3^- had high mass fraction on profiles shown in Fig. 9(a). It was reported that calcium was generally emitted by wear of brake linings, tires (associated with zinc emission), clutch plates and by asphalt road surface mainly in the coarse mode (Monte and Rossi, 2000; Kupiainen *et al.*, 2005). However, it was also considerably emitted from various lubricating oils and diesel powered vehicles in the fine mode (Hopke, 1985). According to emissions from mixed motor vehicles measured in two tunnels in Milwaukee (Lough *et al.*, 2005), PM₁₀ metal emissions were characterized by crustal elements Si, Fe, Ca, Na, etc. Similar results were obtained in a freeway tunnel study in Taiwan (Chiang and Huang, 2009), they reported that SO_4^{2-},

Fig. 8. (a) Oil combustion source profiles obtained at ST3 to ST8, respectively. (b) Time series of corresponding contributions by PMF model.

Fig. 9. (a) Mixed automobile source profiles obtained at ST3 to ST7, respectively. (b) Time series of corresponding contributions by PMF model.

NO_3^-, Ca^{2+}, Na, Fe (presumed to be emitted from mixed automobiles) had high concentrations in/outside the tunnel in fine and coarse fractions as well. In addition, air pollution control regulations by the Korean government had been allowed only a small amount of lead in gasoline since July 1987, unleaded gasoline was completely substituted for leaded gasoline after early 1993. Even though the ambient air quality standard for lead was strengthened from 1.5 μg/m^3/3-month to 0.5 μg/m^3/year in 2001, the annual average lead concentration showed to be satisfactory with a steadily descending trend in the range of 0.304 to 0.008 μg/m^3 during the monitoring period of 1989 to 2007 in this study area (Lee *et al.*, 1995; Kim *et al.*, 1997). Thus, lead and bromine are no longer useful tracers for gasoline emission source in Korea like many other countries. According to Fig. 14(g), the source must be situated northwest from the sampling site. In fact, there have been a densely populated residential area shortly and downtown Suwon City distantly both located northwest from the sampling site. Further campus main gate has been located about 200 m northwest from the sampling site and a 8 lane broad traffic road has been running in front of the gate.

The eighth factor was designated as coal combustion source since NO_3^-, SO_4^{2-}, NH_4^+, Fe, Si, and other trace heavy metals were dominantly observed at ST5 to ST8 (0.4 μm < PM < 3.3 μm). In general fossil fuel combustion emission dominates submicron particles (Seinfeld and Pandis, 1998), but the coal combustion source in this study was partly observed in the coarse particles. It seemed to be

aged and grown during transferring to the receptor. The crustal elements together with various anthropogenic species including SO_4^{2-}, NO_3^-, NH_4^+ were known as markers of coal burning (Hopke, 1985; Chow, 1995; Wilson *et al.*, 2002; Hwang, 2003). After the economic crisis of 1998 in Korea, coal consumption in Korea has been rapidly increased in spite of a regulation for solid fuel restriction in use issued by the Ministry of Environment in 1985. As a matter of fact, a consumption ratio of coal energy to the total energy showed a minimum of 19.3% in 1997 and increased continuously by 22.3% in 2000, 23.8% in 2003, 24.3% in 2006, and 27.4% in 2008, respectively (KEEI, 2009). According to the plots in Fig. 10(b), the source strength was strong during the winter time. The CPF plot for the source in Fig. 14(h) demonstrated direction of this local source located north to northwest from the site similar to oil combustion source. It is noted that Seoul is located almost 30 km north and there had been many scattered small-scale industries using various fossil fuels between Seoul and Suwon.

Secondary aerosol source as the ninth factor was characterized by SO_4^{2-}, NO_3^-, NH_4^+ at ST6 to ST8 (0.4 μm < PM < 2.1 μm). This source was considered to be combined with local and regional sources because it takes time to form particulate SO_4^{2-}, NO_3^-, NH_4^+ from gaseous SO^2, NO^2, NH^3. Once releasing to the ambient, the source exists in the dominant form of NH_4NO_3 and $(NH_4)_xSO_4$ (x = 0 to 2) by homogeneous or heterogeneous photochemical processes (Watson and Chow, 1994; Khoder, 2002; Wilson *et al.*, 2002). Eatough *et al.* (2007) identified 4 secondary sources
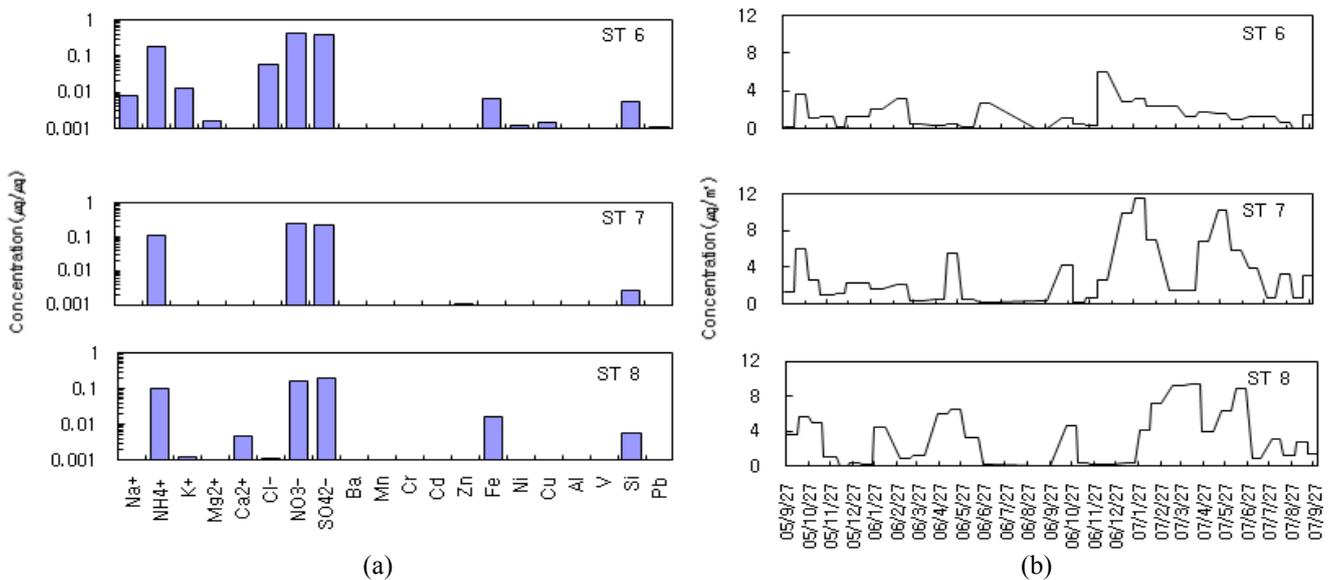
Fig. 10. (a) Coal combustion source profiles obtained at ST5 to ST8, respectively. (b) Time series of corresponding contributions by PMF model.

out of 10 sources using PMF2 in the apportionment study of $PM_{2.5}$ during summer at Pittsburgh. Three of 4 secondary sources were associated with secondary products of local emissions. In general secondary aerosol are actively generated during spring and summer when solar intensity is strong and temperature is high; however, some strong peaks in Fig. 11(b) appeared in the spring of 2006 and the winter of 2007 in our study. The CPF plot in Fig. 14(i) demonstrated the direction of this source located southwest, south-southeast, and north from the monitoring site. According to Table 1, south-southwest wind in spring of 2006 and west-southwest wind in winter of 2007 were

dominant with average wind speed of 2.5 and 1.9 m/sec, respectively.

Incineration source as the tenth factor was characterized by NO_3^-, SO_4^{2-}, Cl^-, NH_4^+, Fe, Zn, Si at ST6 to ST8 (0.4 μm < PM < 2.1 μm) according to species abundances in aerosol mass described in the previous papers (Chow, 1995; U.S.EPA, 1999). The associated emissions were mainly considered from a huge municipal waste incinerator (treating 600 ton/day of waste) located about 2 km northwest from the sampling site. It seemed that it was also influenced by various burning facilities nearby small and mid-size industries.

Fig. 11. (a) Secondary aerosol source profiles obtained at ST6 to ST8, respectively. (b) Time series of corresponding contributions by PMF model.
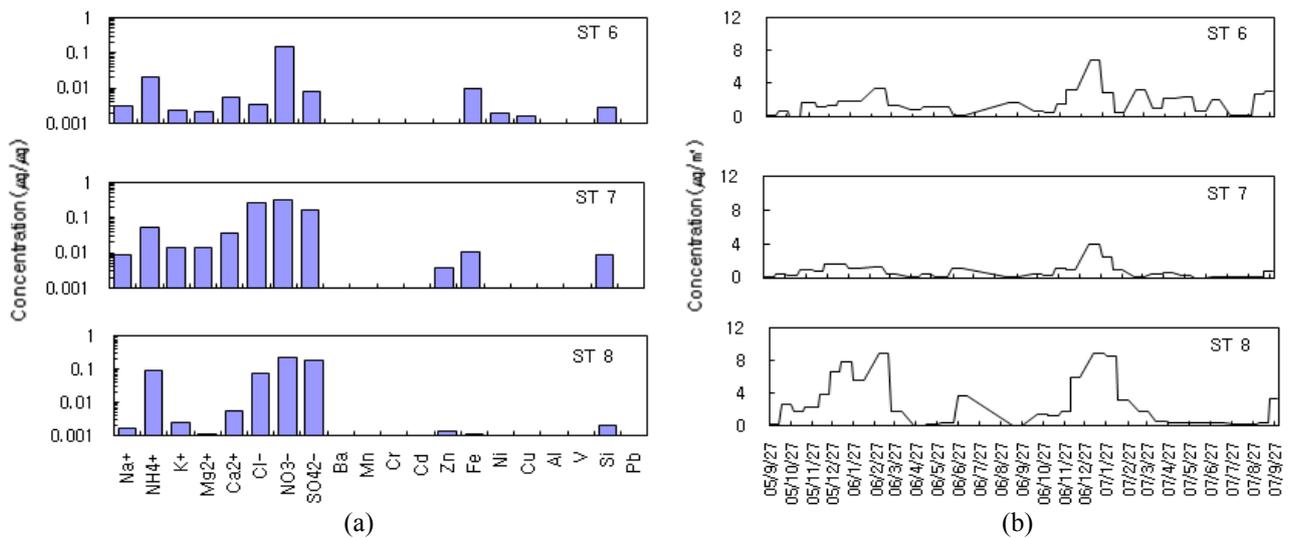
Fig. 12. (a) Incineration source profiles obtained at ST6, ST7, and ST8, respectively. (b) Time series of corresponding contributions by PMF model.
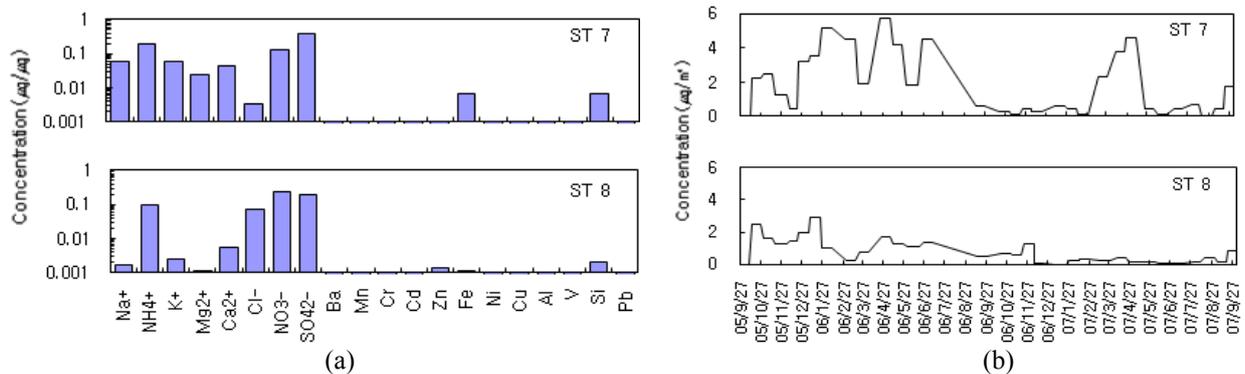
Fig. 13. (a) Biomass burning source profiles obtained at ST7 and ST8, respectively. (b) Time series of corresponding contribution by PMF model.

As the last eleventh factor, biomass burning source was identified by SO_4^{2-}, NO_3^-, NH_4^+, K^+, Ca^{2+}, Na^+, Cl^- at ST7 and ST8 (0.4 μm < PM < 1.1 μm). Similar chemical abundances were reported from agricultural biomass (sugar cane trash) burning in Brazil (Rocha *et al*., 2005) and wintertime biomass burning identified by PMF in Canada (Jeong *et al*., 2008). K^+ is also one of well-known markers for wood burning source (Hopke, 1985; Song *et al*., 2001). From Fig. 14(k), it is noted that various illegal burning activities have been conducted on rural areas located southwest and east from the site.

Consequently, a total of 11 sources were finally extracted even though only 4 to 6 sources were obtained at each stage. As mentioned above, ST9 (backup stage: PM < 0.4 μm) was not involved for PMF. Thus it was difficult to estimate contribution to total aerosol mass including ST9. Nevertheless the average source contributions for two years assorted in specific size ranges could be calculated in Table 6 and average seasonal contributions in Table 7. Seasonal differences were seen in its mass contribution. Long-range transport source was dominated during the springtime by the Asian dust storms. On the whole, aged sea salt, road

dust, long-range transport, and soil sources are most dominant in ST1 (PM > 9.0 μm); mixed automobiles and coal combustion sources in ST5 (2.1 μm < PM < 3.3 μm); oil combustion, secondary aerosol, and incineration in ST8 (0.4 μm < PM < 0.7 μm); and biomass burning source in ST7 (0.7 μm < PM <1.1 μm), respectively. Major contributors at this site were long-range transport source from the southwest, secondary aerosol source from the southwest and south-southeast, and mixed automobile source from the northwest by contribution sequence.

CONCLUSIONS

A total of 32 sets of PM samples were collected for two years by a 9-stage cascade impactor at an urbanized local site in Korea. The 20 chemical species in PM were analyzed by ICP-AES and IC. Based on the chemical data (except data from backup stage), PMF was used to identify PM sources and CPF was used to examine the potential location of the identified sources. Major contributors at the sampling site were long-range transport source from the southwest, secondary aerosol source from the southwest
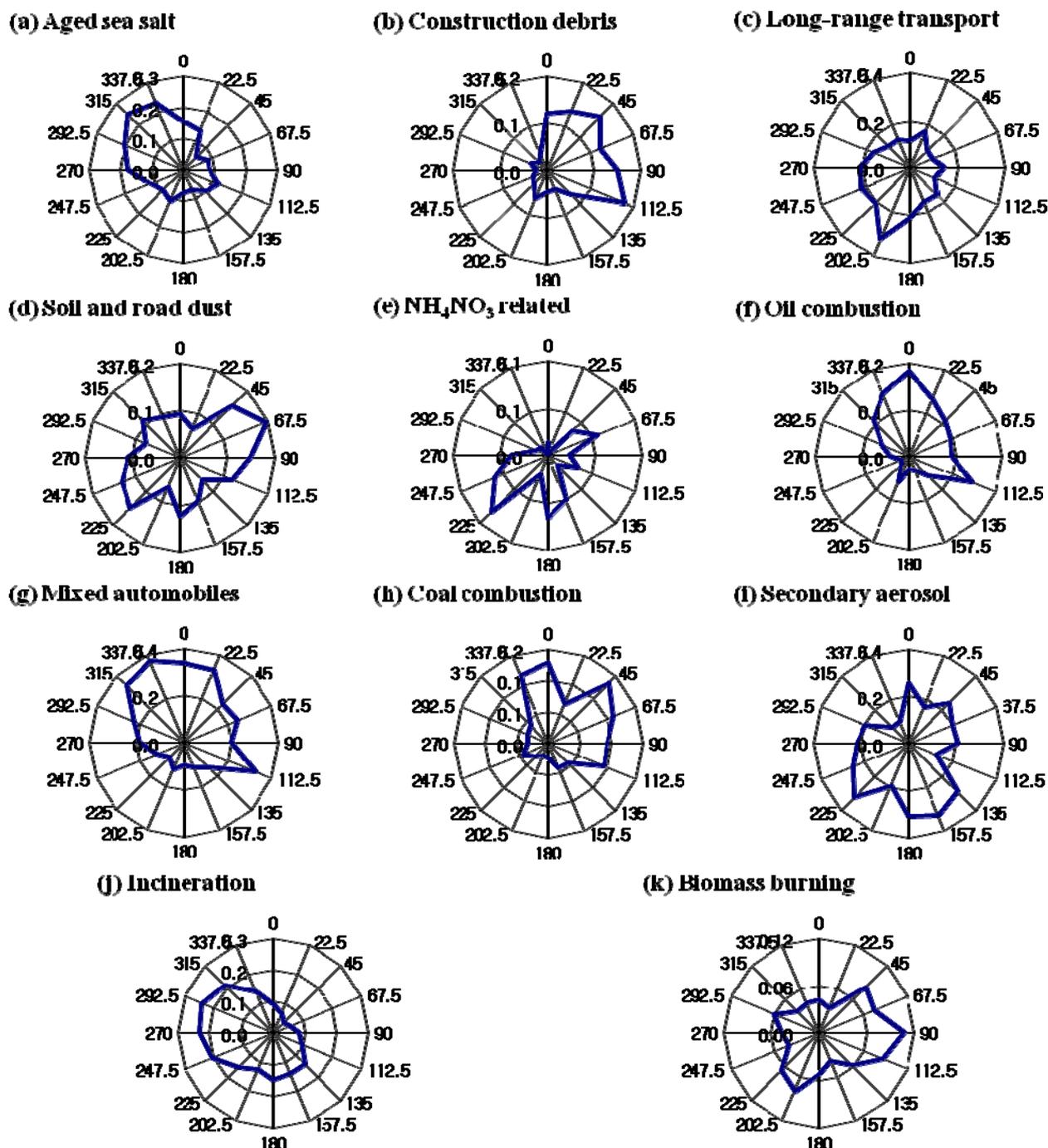
Fig. 14. The CPF plots of the contribution at sampling site.

and south-southeast, and mixed automobile source from the northwest. On the other hand the building debris source as a minor was identified near the site. The relative contribution of most abundant sources was 32.4% of long-range transport source in the coarse particle mode and 34.5% of secondary aerosol in the fine particle mode, respectively.

The source apportionment study based on size segregation was useful to control specific emission sources in local area, to assess their impacts on health and wealth, and further to examine size-resolved aerosol compositions from them.

Above all benefits obtained from PMF study, the size-resolved analysis provided most useful information when classifying statistically undefined sources into potentially defined sources by examining temporal dependence and distribution of contributions at nearby particle size ranges.

For further studies to understand more detailed local/regional emission sources, it is necessary to expand more chemical variables such as temperature-resolved carbon compounds and the other inorganic elements, to develop more marker species for specific sources, and to improve quality assurance and quality control.

Table 7. A comparison of seasonal source contributions to the aerosol mass with particle size larger than 0.4 μm.

Season	Aged sea salt	Construction debris	Long-range transport	Soil and road dust	NH$_4$NO$_3$ related	Oil Combustion	Mixed automobiles	Coal combustion	Secondary aerosol	Incineration	Biomass burning	Total
Spring	6.3 (8.9%)	0.2 (0.3%)	20.4 (28.8%)	4.2 (5.9%)	3.0 (4.3%)	2.6 (3.6%)	8.1 (11.4%)	7.5 (10.5%)	10.5 (14.7%)	4.1 (5.7%)	4.0 (5.7%)	71.0 (100%)
Summer	1.5 (4.0%)	0.7 (1.8%)	5.6 (14.9%)	4.5 (11.9%)	3.2 (8.5%)	3.3 (8.9%)	3.3 (8.7%)	5.5 (14.7%)	6.5 (17.3%)	1.7 (4.5%)	1.8 (4.8%)	37.6 (100%)
Fall	6.7 (14.5%)	0.4 (0.9%)	5.6 (12.1%)	3.6 (7.8%)	2.3 (5.0%)	2.9 (6.4%)	8.4 (18.1%)	5.8 (12.5%)	5.4 (11.7%)	3.2 (6.9%)	1.9 (4.0%)	46.4 (100%)
Winter	7.3 (11.3%)	0.2 (0.3%)	9.2 (14.3%)	5.5 (8.5%)	3.0 (4.6%)	1.5 (2.3%)	8.7 (13.5%)	6.8 (10.5%)	9.3 (14.5%)	10.4 (16.1%)	2.7 (4.2%)	64.4 (100%)

REFERENCES

Anlauf, K., Li, S.M., Leaitch, R., Brook, J., Hayden, K., Toom-Sauntry, D. and Wiebe, A. (2006). Ionic Composition and Size Characteristics of Particles in the Lower Fraser Valley: Pacofoc 2001 Field Study. *Atmos. Environ.* 40: 2662–2675.

Appel, B.R., Tokiwa, Y., Hsu, J., Kothny, E.L. and Hann, E. (1985). Visibility as Related to Atmospheric Aerosol Constituents. *Atmos. Environ.* 20: 1969–1977.

Ashbaugh, L.L., Malm,.C. and Sadeh, W.D. (1985). A Residence Time Probability Analysis of Sulfur Concentrations at Grand Canyon National Park. *Atmos. Environ.* 19: 1263–1270.

Chiang, H. and Huang, Y. (2009). Particulate Matter Emissions from On-road Vehicles in a Freeway Tunnel Study. *Atmos. Environ.* 43: 4014–4022.

Chow, J.C. (1995). Measurement Methods to Determine Compliance with Ambient Air Quality Standards for Suspended Particles. *J. Air Waste Manage. Assoc.* 45: 320–382.

Eatough, E.J., Mangelson, N.F., Anderson, R.R., Martello, D.V., Pekney, N.J., Davidson, C.I. and Modey, W.K. (2007). Apportionment of Ambient Primary and Secondary Fine Particulate Matter during a 2001 Summer Intensive Study at the CMU Supersite and NETL Pittsburgh Site. *J. Air Waste Manage. Assoc.* 57: 1251–1267.

EPA. (1999). SPECIATE Ver 3.1.

Feng, Y. and Penner, J. (2007) Global Modeling of Nitrate and Ammonium: Interaction of Aerosols and Tropospheric Chemistry. *J. Geophys. Res.* 112: D01304, doi: 10.1029/2005JD006404.

Guerra, S.A., Lane, D.D., Marotz, G.A., Carter, R.E., Hohi, C.M. and Baldauf, R.W. (2006). Effects of Wind Direction on Coarse and Fine Particulate Matter Concentrations in Southeast Kansas. *J. Air Waste Manage. Assoc.* 56: 1525–1531.

Han, J.S., Moon, K.J., Kim, R.H., Shin, S.A., Hong, Y.D. and Jung, I.R. (2006b). Preliminary Source Apportionment of Ambient VOCs Measured in Seoul Metropolitan Area by Positive Matrix Factorization. *J. Korean Soc. Atmos. Environ.* 22: 85–97.

Han, J.S., Moon, K.J., Lee, S.J., Kim, Y.J., Ryu, S.Y., Cliff, S.S. and Yi, S.M. (2006). Size-resolved Source Apportionment of Ambient Particles by Positive Matrix Factorization at Gosan Background Site in East Asia. *Atmos. Chem. Phys.* 6: 211–223.

Hidy, G.M. (1972). *Aerosols and Atmospheric Chemistry*, Academic Press, New York.

Hopke, P.K. (1985). *Receptor Modeling in Environmental Chemistry*, John Wiley & Sons.

Hopke, P.K. (2000). A Guide to Positive Matrix Factorization, in workshop on UNMIX and PMF as applied to PM$_{2.5}$. Edited by R.D. Willis, RTP, NC, EPA 600/A-00/048.

Hwang, H. and Ro, C.U. (2006) Direct Observation of Nitrate and Sulfate Formations from Mineral Dust and Sea-salts Using low-Z Particle Electron Probe X-ray Microanalysis. *Atmos. Environ.* 40: 3869–3880.

Hwang, I.J. and Kim, D.S. (2003). Estimation of Quantitative Source Contribution of Ambient PM$_{10}$ Using the PMF Model. *J. Korean Soc. Atmos. Environ.* 19: 719–731.

Hwang, I.J., Bong, C.K., Lee, T.J. and Kim, D.S. (2002). Source Identification and Quantification of Coarse and Fine Particles by TTFA and PMF. *J. Korean Soc. Atmos. Environ.* 18: 203–213.

Hwang, I.J., Kim, T.O. and Kim, D.S. (2001). Source Identification of PM-10 in Suwon Using the Method of Positive Matrix Factorization. *J. Korean Soc. Atmos. Environ.* 17: 133–145.

Jeong, C.H., Evans, G.J., Dann, T., Graham, M., Herod, D., Dabeck-Zlotorzynska, E., Mathieu, D., Ding, L. and Wang, D. (2008). Influence of Biomass Burning on Wintertime Fine Particulate Matter; Source Contribution at a Valley Site in Rural British Columbia. *Atmos. Environ.* 42: 3684–3699.

John, W., Wall, S.M., Ondo, J.L. and Winklmayr, W. (1990). Modes in the Size Distribution of Atmospheric Inorganic Aerosol. *Atmos. Environ.* 24A: 2349–2359.

Jonson, J.E., Barrett, A.K., Grini, A. and Tarrason, L. (2000). On the Distribution of Sea Salt and Sodium Nitrate Particles in Europe, Transport and Chemical Transportation in the Troposphere. Proceedings of the EUROTRAC Symposium, 6th, Gaimisch-Partenkirchen, Germany, 27–31 March 2000, p. 695–699.

Kang, B.W., Kang, C.M., Lee, H.S. and Sunwoo, Y. (2008) Identification of Potential Source Locations of $PM_{2.5}$ in Seoul Using Hybrid-receptor Models. *J. Korean Soc. Atmos. Environ.* 24: 662–673.

KEEI. (2009). *Korea Energy Economics Institute, 2009. Yearbook of Energy Statistics*, ISSN 1226-606X. Ministry of Knowledge Economy, Korea.

Khoder, M.I. (2002). Atmospheric Conversion of Sulfur Dioxide to Particulate Sulfate and Nitrogen Nitric Acid in an Urban Area. *Chemosphere* 49: 675–684.

Kim, D.S. (2009). The Past, Present, and Future of Atmospheric Science and Technology in Korea. *J. Korean Soc. Atmos. Environ.* 25(6).

Kim, D.S. and Lee, T.J. (1993). Quantitative Source Estimation of Particulate Matters in Suwon Area Using the TTFA Based on Size Segregation Scheme. *J. Korean Air Pollut. Res. Assoc.* 9: 44–50.

Kim, E. and Hopke, P.K. (2004a). Source Apportionment of Fine Particles in Washington, DC, Utilizing Temperature-resolved Carbon Fractions. *J. Air Waste Manage. Assoc.* 54: 773–785.

Kim, E. and Hopke, P.K. (2004b). Improving Source Identification of Fine Particles in a Rural Northeastern US Area Utilizing Temperature Resolved Carbon Fractions. *J. Geophys. Res.* 109: D09204.

Kim, E. and Hopke, P.K. (2004d). Comparison between Conditional Probability Function and Nonparametric Regression for Fine Particle Source Directions. *Atmos. Environ.* 38: 4667–4673.

Kim, E., Hopke, P.K. and Edgerton, E.S. (2004c). Improving Source Identification of Atlanta Aerosol Using Temperature Resolved Carbon Fractions in Positive Matrix Factorization. *Atmos. Environ.* 38: 3349–3362.

Kim, E., Larson, T.V., Hopke, P.K., Slaughter, C., Sheppard, L.E. and Claibom, C. (2003). Source Identification of $PM_{2.5}$ in an Arid Northwest U.S. City by Positive Matrix Factorization. *Atmos. Res.* 66: 291–305.

Kim, K.H., Kim, D.S. and Lee, T.J. (1997). The Temporal Variabilities in the Concentrations of Airborne Lead and its Relationship to Aerosol Behavior. *Atmos. Environ.* 31: 3449–3458.

Kim, S.D., Kim, D.S., S.Y. Cho., Kim, Y.J. and Lee, J.J. (2006) (Nov). Investigation of Ambient PM_{10} Generation Processes and Establishment of Its Reduction Strategies. Final Report for Study on Air Quality Management Plans in Seoul Metropolitan Area. *National Institute of Environmental Research*.

Kim, T.O., Kim, D.S. and Na, J.G. (1990). Quantitative Source Estimation of Particulate Matters in Busan Area Using TTFA. *J. Korean Air Pollut. Res. Assoc.* 6: 135–146.

KMA. (2006–2008). *Korea Meteorological Administration, 2006–2008*, Meteorological Phenomena.

Kupiainen, K.J., Tervahattu, H., Raisanen, M., Makela, T., Aurela, M. and Hillamo, R. (2005). Size and Composition of Airborne Particles from Pavement Wear, Tires, and Traction Sanding. *Environ. Sci. Technol.* 39: 699–706.

Lee, E., Chan, C.K. and Paatero, P. (1999). Application of Positive Matrix Factorization in Source Apportionment of Particulate Pollutants in Hong Kong. *Atmos. Environ.* 33: 3201–3212.

Lee, J.H., Youshida, Y., Turpin, B.J., Hopke, P.K., Poirot, R.L., Lioy, P.J. and Oxley, J.C. (2002). Identification of Sources Contributing to Mid-Atlantic Regional Aerosol. *J. Air Waste Manage. Assoc.* 52:1186–1205.

Lee, S. and Russell, A.G. (2007). Estimating Uncertainties and Uncertainty Contributors of CMB $PM_{2.5}$ Source Apportionment Results. *Atmos. Environ.* 41: 9616–9624.

Lee, S., Liu, W., Wang, Y., Russell, A.G. and Edgerton, E.S. (2008). Source Apportionment of $PM_{2.5}$: Comparing PMF and CMB Results for Four Ambient Monitoring Sites in the Southeastern United States. *Atmos. Environ.* 42: 4126–4137.

Lee, T.J., Kim, S.C. and Kim, D.S. (1995). Determination of Atmospheric Lead in Suwon City. *Journal of Korean Environmental Sciences Society* 5: 535–542.

Lewis, E.R. and Schwartz, S.E. (2004). *Sea Salt Aerosol Production: Mechanisms, Methods, Measurements, and Models*, AGU.

Lough, G.C., Schauer, J.J., Park, J.S., Shafer, M.M., Deminter, J.T. and Weinstein, J.P. (2005). Emissions of Metals Associated with Motor Vehicle Roadways. *Environ. Sci. Technol.* 39: 826–836.

Monte, M.D. and Rossi, P. (2000). *Calcium in the Urban Atmosphere, in Aerosol Chemical Processes in the Environment*, Spurny, K.R. (Ed.), Lewis Publishers, New York.

Morawska, L. and Zhang, J. (2002). Combustion Sources of Particles. 1. Health Relevance and Source Signatures. *Chemosphere* 49: 1045–1058.

Mori, I., Nishikawa, M., Tanimura, T. and Quan, H. (2003). Change in size distribution and chemical composition of kosa (Asian dust) aerosol during long-range transport. *Atmos. Environ.* 37: 4253–4263.Oh, M.S., Lee, T.J. and Kim, D.S. (2009). Source Identification of Ambient Size-by-size Particulate Using the Positive Matrix Factorization Model on the Border of Yongin and Suwon. *J. Korean Soc. Atmos. Environ.* 25: 108–121.

Paatero, P. and Tapper, U. (1994). Positive Matrix Factorization: A Non-negative Factor Model with Optimal Utilization of Error Estimates of Data Values. *Environmetrics* 5: 111–126.

Polissar, A.V., Hopke, P.K. and Poirot, R.D. (2001). Atmospheric Aerosol over Vermont: Chemical Composition and Sources. *Environ. Sci. Technol.* 35: 4604–4621.

Polissar, A.V., Hopke, P.K., Paatero, P., Malm, W.C. and Sisler, J.F. (1998). Atmospheric Aerosol over Alaska, 2. Elemental Composition and Sources. *J. Geophys. Res.* 103: 19045–19057.

Pope, C.A., Bates, D.V. and Raizenne, M.E. (1995). Health Effects of Particulate Air Pollution: Time for Reassessment. *Environ. Health Perspect.* 103: 472–480.

Qin, Y. (2005). Estimation of Organic Carbon Blank Values and Error Structures of the Speciation Trend Network Data for Source Apportionment. *J. Air Waste Manage. Assoc.* 55: 1190–1199.

Ramadan, Z., Song, X.H. and Hopke, P.K. (2000). Identification of Sources of Phoenix Aerosol by Positive Matrix Factorization. *J. Air Waste Manage. Assoc.* 50: 1308–1320.

Rocha, C.O., Allen, A.G. and Cardoso, A.A. (2005). Influence of Agricultural Biomass Burning on Aerosol Size Distribution and Dry Deposition in Southeastern Brazil. *Environ. Sci. Technol.* 39: 5293–5301.

Schroeder, W.H., Dobson, M., Kane, D.M. and Johnson, N.D. (1987). Toxic Trace Elements Associated with Airborne Particulate Matter: A Review. *J. Korean Air Pollut. Res. Assoc.* 37: 1267–1285.

Schwartz, J. and Dockery, D.W. (1992). Increased Mortality in Philadelphia Associated with Daily Air Pollution Concentrations. *Am. Rev. Respir. Dis.* 145: 600–604.

Seinfeld, J.H. and Pandis, S.P. (1998). Atmospheric Chemistry and Physics, John Wiley & Sons.

Shin, S.A., Han, J.S. and Kim, S.D. (2006) Source Apportionment and the Origin of Asian Dust Observed in Korea by Receptor Modeling (CMB). *J. Korean Soc. Atmos. Environ.* 22: 157–166.

Song, X.H., Polissar, A.V. and Hopke, P.K. (2001). Source of Fine Particle Composition in the Northeastern US. *Atmos. Environ.* 35: 5277–5286.

Suwon City. (2010). http://eng.suwon.ne.kr/sub/happy_uwon/happy_02_01.asp?menuCode=0102.

Takahashi, H., Naoe, H., Igarashi, Y., Inomata, Y. and Sugimoto, N. (2010). Aerosol Concentrations Observed at Mt. Haruna, Japan, in Relation to Long-range Transport of Asian Mineral Dust Aerosols. *Atmos. Environ.* 44: 4638e4644.U.S.

Watson, J.G. and Chow, J.C. (1994). Ammonium Nitrate, Nitric Acid and Ammonia Equilibrium in Wintertime Phoenix Arizona. *J. Air Waste Manage. Assoc.* 44: 405–412.

Wilson, W.E., Chow, J.C., Claiborn, C., Fusheng, W., Engelbrecht, E.J. and Watson, J.G. (2002). Monitoring of Particulate Matter Outdoors. *Chemosphere* 49: 1009–1043.

Yongin City. (2010). http://en.yonginsi.net/cms.asp?code=E1010010.